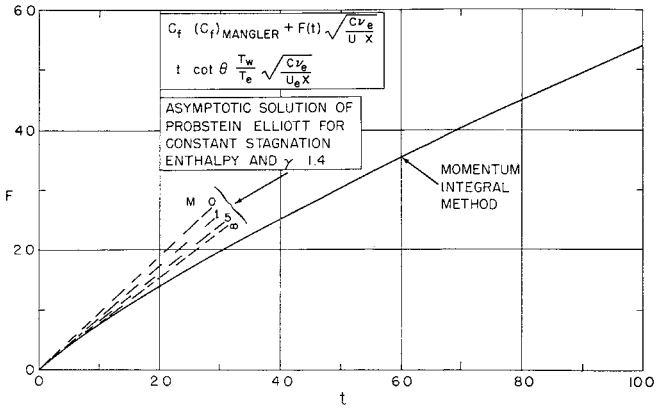

Fig 1 Transverse-curvature correction on the Mangler skin-friction coefficient for a cone

3 Discussion

It now is possible to arrive at an estimate of the accuracy of the present method, at least in the regime of weak curvature effects, by comparing Eq (7) with the asymptotic expansion of Probstein and Elliott [1] If we assume a constant stagnation enthalpy throughout the boundary layer (which corresponds to an insulated wall and a Prandtl number of unity), it follows from Eq (7) for the local skin-friction coefficient that

$$C_f = \left(\frac{C\nu_e}{u\,x}\right)^{1/2} + 0\,80\,\cot\theta\left(1 + \frac{\gamma - 1}{2}\,Me^2\right)\frac{C\nu_e}{u_e x} + \tag{9}$$

The corresponding solution of Probstein and Elliott is

$$C_f = 1\,15\left(\frac{C\nu_e}{u\,x}\right)^{1/2} + \cot\theta\left(0\,95 + 0\,77\,\frac{\gamma - 1}{2}\,Me^2\right)\frac{C\nu_e}{u_e x} + \tag{10}$$

The leading term of Eq (9) is the flat-plate result as obtained with a straight-line profile, multiplied by the Mangler factor $3^{1/2}$ This term is in error by about 13% compared with the leading term of Eq (10), the latter being the Chap man-Rubesin flat-plate expression multiplied by the same Mangler factor The deviation of the incompressible part of the second term in Eq (9) amounts to almost 16% However, for increasing Mach numbers, the compressible part of the second term, being in error by about 4%, will gradually dominate

In Fig 1 the function $F(t)$ is compared with the asymptotic solution of Probstein and Elliott for the case of constant stagnation enthalpy and $\gamma = 1\,4$

For hypersonic flow over a very slender insulated cone, it follows approximately from Eq (6) that

$$t \propto \frac{Me^2}{\theta}\left(\frac{C\nu_e}{u\,x}\right)^{1/2} = \frac{\chi}{K} \tag{11}$$

where $\chi = C^{1/2}M^3/(Re_x)^{1/2}$ is the local hypersonic viscous interaction parameter, and $K = M_e\theta$ is the local hypersonic similarity parameter In many cases of practical interest, K will be of the order of unity

It should be kept in mind, however, that the present analysis is based on the assumption of constant pressure throughout the boundary layer Consequently, the effect of the self-induced pressure distribution on the boundary-layer development has not been accounted for

The momentum-integral analysis sketched in the preceding paragraphs is readily extended[2] to include (slender) bodies of revolution of the type $r_w \propto x^n$, provided that pressure gradients along the body are neglected In that case we employ the more general transverse curvature parameter

$$t = \frac{\cos\theta}{r_w}\,\frac{T_w}{T_e}\left(\frac{C\,\nu_e\,x}{u_e}\right)^{1/2}$$

and we find, as in Eq (5), that the local skin-friction coefficient equals its Mangler value multiplied by a function which depends on the parameter t only It is further easily verified that, for a slender insulated power-law body, relation (11) still holds true

References

[1] Probstein, R F and Elliott, D , "The transverse curvature effect in compressible axially symmetric laminar boundary-layer flow," J Aerospace Sci **23,** 208–224, 236 (1956)

[2] Raat, J , "On the effect of transverse curvature in com pressible boundary-layer flow over slender bodies of revolution," U S Naval Ordnance Lab TR 63-68 (1964)

[3] Glauert, M B and Lighthill, M J , "The axisymmetric boundary layer on a long thin cylinder,' Proc Roy Soc (London) **230,** 188–203 (1955)

Heat Transfer Due to Hydromagnetic Channel Flow with Conducting Walls

K JAGADEESAN*
Indian Institute of Technology, Kharagpur, India

Nomenclature

μ	=	magnetic permeability
σ	=	electrical conductivity of the fluid
$\mathbf{H}$	=	magnetic field vector
H_y	=	applied magnetic field
$\mathbf{J}$	=	current density
$\mathbf{E}$	=	electric field
$\mathbf{q}$	=	velocity of the fluid
ρ	=	density of the fluid
c	=	velocity of light
η	=	electrical diffusivity $= (1/\sigma)c^2/(4\pi\mu)$
ν	=	kinematic viscosity
p_m	=	magnetic Prandtl number $= \eta/\nu$
a	=	Alfven's wave velocity $= (\mu H_y^2/4\pi\rho)^{1/2}$
R_m	=	magnetic Reynold s number $= aL/\nu$
M	=	Hartmann number $= aL(\eta\nu)^{-1/2}$
σ_{w1}, σ_{w2}	=	conductivity of the lower and upper walls
h_1, h_2	=	thickness of the lower and upper walls
ϕ_1, ϕ_2	=	electrical conductance parameters of the lower and upper walls
c_p	=	specific heat
K	=	thermal conductivity of the fluid
E_m	=	magnetic Eckert's number $= a^2/c_p\theta_1$
P	=	Prandtl number $= \mu c_p/K$
L	=	channel half width

THE problem of the two-dimensional flow of an incompressible, viscous, and electrically conducting fluid through a channel formed by two parallel nonconducting walls subjected to the action of uniform transverse magnetic field in the presence of heat transfer was considered in Refs 1–3 The first reference contained a solution for a uniform heat flux without considering viscous dissipation However, in the second reference, the effect of viscous dissipation was taken into account In Ref 3 the problem

Received October 14, 1963 The author is much obliged to M K Jain and J P Agarwal for their kind guidance and assistance

* Research Scholar, Department of Mathematics

Table 1 Variation in Nusselt number with the increase in $\phi_1 + \phi_2$ for $\lambda_1 = 10$, $\lambda_2 = 1$

$(\phi_1 + \phi_2)$	$M = 1$	$M = 2$	$M = 3$	$M = 4$	$M = 5$	$M = 6$
0	5 0018	5 5984	6 5705	7 9030	9 5995	11 6920
3	3 6801	2 6699	2 2615	2 0955	2 0216	1 9869
6	3 3930	2 4078	2 0669	1 9458	1 8999	1 8835
9	3 2768	2 3141	2 0092	1 9049	1 8686	1 8582
∞	3 0086	2 1441	1 9103	1 8406	1 8227	1 8212

considered in Refs 1 and 2 has been generalized, and the relation $T = \tau x + \theta(y)$ has been used

The purpose of this note is to study the effect of wall conductance on the steady, incompressible, hydromagnetic, fully developed channel flow in the presence of heat transfer

With the assumptions

$$\mathbf{q} = u\mathbf{i} + v\mathbf{j} \qquad \mathbf{H} = H_x\mathbf{i} + H_y\mathbf{j}$$
$$p = p(x,y) \qquad T = \tau x + \theta(y) \tag{1}$$

the governing equations are

$$\nu \frac{d^2u}{dy^2} + \frac{\mu_e}{4\pi\rho} H_y \frac{dH_x}{dy} = \frac{1}{\rho}\frac{dP}{dx} \tag{2}$$

$$\eta \frac{d^2H_x}{dy^2} + H_y \frac{du}{dy} = 0 \tag{3}$$

and

$$\rho c_p \tau u = K\frac{d^2\theta}{dy^2} + \mu\left(\frac{du}{dy}\right)^2 + \frac{c^2}{16\pi^2\sigma}\left(\frac{dH_x}{dy}\right)^2 \tag{4}$$

where $[p + (\mu H_x^2/8\pi)] = P$ Using the transformations

$$\bar{u} = \frac{u}{a} \qquad \bar{H}_x = \frac{H_x}{H_y} \qquad \xi = \frac{y}{L}$$
$$\bar{P} = -\frac{1}{\rho\nu^2 L^{-3}}\frac{dP}{dx} \qquad \bar{\theta} = \frac{\theta}{\theta_1} \tag{5}$$

into Eqs (2–4), we get

$$\frac{d^2\bar{u}}{d\xi^2} + R_m \frac{d\bar{H}_x}{d\xi} = -\frac{\bar{P}}{R_m} \tag{6}$$

$$p_m \frac{d^2\bar{H}_x}{d\xi^2} + R_m \frac{d\bar{u}}{d\xi} = 0 \tag{7}$$

and

$$P\,R_m s\bar{u} = \frac{d^2\bar{\theta}}{d\xi^2} + P\,E_m\left[\left(\frac{d\bar{u}}{d\xi}\right)^2 + p_m\left(\frac{d\bar{H}_x}{d\xi}\right)^2\right] \tag{8}$$

where the parameter $s = \tau L/\theta_1$ The boundary conditions are

$$\bar{u} = 0 \qquad \text{at } \xi = \pm 1 \tag{9}$$

$$\bar{\theta} = 0 \qquad \text{at } \xi = \pm 1 \tag{10}$$

$$\frac{d\bar{H}_x}{d\xi} - \frac{1}{\phi_1}\bar{H}_x = 0 \qquad \text{at } \xi = -1 \tag{11}$$

and

$$\frac{d\bar{H}_x}{d\xi} + \frac{1}{\phi_2}\bar{H}_x = 0 \qquad \text{at } \xi = +1 \tag{12}$$

where

$$\phi_1 = \frac{\sigma_{w_1}h_1}{\sigma L} \qquad \phi_2 = \frac{\sigma_{w_2}h_2}{\sigma L} \tag{13}$$

Solutions of Eqs (6) and (7) with the boundary conditions (9, 11, and 12) as given in Ref 4 are

$$\frac{R_m}{\bar{P}}\bar{u} = \frac{\Phi_1}{M}\left[\coth M - \frac{\cosh M\xi}{\sinh M}\right] \tag{14}$$

$$\frac{R_m^2}{\bar{P}}\bar{H}_x = \left[\frac{\Phi_1 \sinh M\xi}{\sinh M} + \Phi_2\left(\frac{1}{M} - \coth M\right) - \xi\right] \tag{15}$$

where Φ_1 and Φ_2 represent the ratios

$$\Phi_1 = \frac{(\phi_1 + \phi_2 + 2)}{(\phi_1 + \phi_2)M\coth M + 2}$$
$$\Phi_2 = \frac{(\phi_2 - \phi_1)M}{(\phi_1 + \phi_2)M\coth M + 2} \tag{16}$$

Substituting Eqs (14) and (15) into Eq (8) we get

$$\frac{d^2\bar{\theta}}{d\xi^2} = \frac{\lambda_2\Phi_1}{M}\left[\coth M - \frac{\cosh M\xi}{\sinh M}\right] - \frac{\lambda_1}{M^2\sinh^2 M} \times$$
$$[\Phi_1^2 M^2\cosh 2M\xi - 2\phi_1 M\sinh M\cosh M\xi + \sinh^2 M] \tag{17}$$

where the nondimensional heat-transfer parameters λ_1 and λ_2 are given by

$$\lambda_1 = PrE_m\frac{\bar{P}^2}{R_m^2} \qquad \lambda_2 = P\,s\bar{P} \tag{18}$$

Integrating (17) twice, and applying the boundary condition (10), we obtain

$$\bar{\theta} = \frac{\lambda_1}{M^2\sinh^2 M}\left[\frac{\Phi_1^2}{4}(\cosh 2M - \cosh 2M\xi) - \frac{2\Phi_1}{M}(\sinh M)(\cosh M - \cosh M\xi) + \frac{1}{2}(1 - \xi^2)\sinh^2 M\right] + \frac{\lambda_2\Phi_1}{M} \times$$
$$\left[\frac{1}{M^2\sinh M}(\cosh M - \cosh M\xi) - \frac{1}{2}(1 - \xi^2)\coth M\right] \tag{19}$$

The Nusselt number N is defined by

$$N = -\frac{L}{\theta(0)}\left(\frac{\partial T}{\partial y}\right)_{y=L} = -\frac{1}{\bar{\theta}(0)}\left(\frac{d\bar{\theta}}{d\xi}\right)_{\xi=1} \tag{20}$$

which leads to

$$N = \frac{\lambda_2\Phi_1(M\coth M - 1) - \lambda_1(\Phi_1^2 M\coth M - 2\Phi_1 + 1)}{\lambda_1\left[\frac{\Phi_1^2 + 1}{2} - \frac{2\Phi_1}{M}\tanh\frac{M}{2}\right] + \lambda_2\Phi_1\left[\frac{1}{M}\tanh\frac{M}{2} - \frac{1}{2}M\coth M\right]} \tag{21}$$

Table 1 and Fig 1 give the Nusselt number and the temperature profiles, respectively, for different value of M and $(\phi_1 + \phi_2)$

From the table and the figure the following conclusions are made The Nusselt number is the same at the lower and upper walls whether ϕ_1 and ϕ_2 are equal or different, and it decreases with the increase in $(\phi_1 + \phi_2)$ It depends only upon the

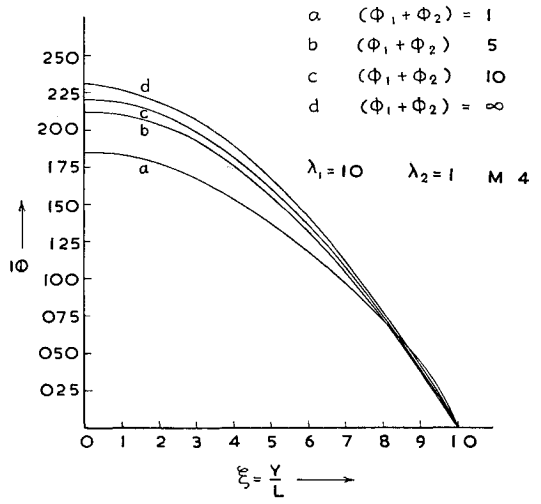

Fig 1 Temperature distribution for the values of ($\phi_1 + \phi_2$) indicated

sum ($\phi_1 + \phi_2$) and not upon the individual values of ϕ_1 and ϕ_2

The temperature profiles are symmetric about the middle of the channel and depend only upon the sum ($\phi_1 + \phi_2$) These profiles decrease when ($\phi_1 + \phi_2$) increases from zero to ϕ_T and increase for ($\phi_1 + \phi_2$) > ϕ_T where ϕ_T is the transitional value given by

$$\frac{\phi_T + 2}{\phi_T M \coth M + 2} = \frac{\left[\frac{2\sinh M}{M}(\cosh M - \cosh M\xi)(2\lambda_1 - \lambda_2) + \lambda_2 M(1 - \xi^2)\sinh M \cosh M\right]}{\lambda_1(\cosh 2M - \cosh 2M\xi)}$$

References

[1] Siegel, R, "Heat transfer in swirling laminar pipe flow," J Appl Mech **25,** 295–296 (1958)

[2] Regirer, S A, "Concerning the thermal effect in the flow of an electrically conducting fluid between parallel walls," J Appl Math Mech **23,** 1346–1350 (1959)

[3] Zimin, E P, "The flow of a viscous, electrically conducting g as in a transverse magnetic field in the presence of heat transfer" J Appl Math Mech **25,** 566–568 (1961)

[4] Chang, C C and Yen, J T, "Hydromagnetic channel flow with conducting walls," Z Angew Math Phys **XIII,** 266–272 (1962)

Effect of Radiation on Upper Limits of Inflammability

Beshir A Abbadi* and Richard S Tankin†
Northwestern University, Evanston, Ill

THE study of the limits of inflammability is of importance, not only for minimizing the risk of fires and explosions, but also for a better understanding of the principles of flame propagation For many years, the existence of upper and lower limits of inflammability have been known There have been several efforts to predict these limits analytically,[1,2] but these theories have met with limited success

Egerton and Powling[3] have investigated the effects of radiation losses on upper and lower limits of hydrogen-oxygen mixtures The wall of the combustion tube was blackened in one set of experiments and silvered in another; there was very little difference in the results (less than 0 3% for upper limit) In this note, it is shown experimentally that the upper limit of a propane-air mixture is significantly affected by radiation losses

Received December 23, 1963

* Graduate Student
† Assistant Professor

Experimental Apparatus

The U S Bureau of Mines has standardized the experimental procedure for determining the upper limit of inflammability as follows[4]:

The mixture to be tested is contained in a vertical glass tube of not less than 2″ in diameter and not less than 4′ 6″ long The tube is closed at the top and at the moment of testing is opened at the lower end and a naked flame $\frac{3}{4}$″ to 1″ long is applied If the flame propagates the entire length of the tube, the mixture is judged to be inflammable but not otherwise

The richest fuel-air mixture, at which uniform propagation occurs, defines the upper limit of inflammability

The combustion tube used in this study was a Pyrex tube with a 2-in i d and 4 ft 11 in long There were provisions for evacuating the combustion tube, introducing the test mixture, and mixing the fuel and air A schematic drawing of the apparatus is shown in Fig 1 The top of the combustion tube was closed with an air-tight glass plug A flat piece of glass with a rubber gasket and a mercury seal was used to close the lower end of the combustion tube when evacuating the combustion tube, filling it with fuel and air, and during the mixing of fuel and air Instrument grade propane, having a minimum purity of 99 5%, and dry air were used in the experiments A manometer was used to read the pressure within the combustion tube and, hence, to determine the composition of the mixture In one set of experiments, a gold-coated front-surfaced mirror with a diameter of $2\frac{1}{8}$ in was placed $\frac{1}{2}$ in below the lower end of the combustion tube

Test Procedure

The following experiments were conducted to determine the upper limits of inflammability for propane-air mixtures:

Case I Combustion tube is uncoated, glass plug at upper end of tube is uncoated, and lower end of tube is open to the atmosphere This is the standard test as specified by the U S Bureau of Mines

Case II: The inner surface of the combustion tube is silver coated, the glass plug at the upper end of tube is uncoated, and lower end of tube is open to the atmosphere This experimental setup is similar to that used by Egerton and Powling

Case III The inner surface of the combustion tube is silver coated, the inner surface of the plug at the upper end of the tube is silver coated, and a spherical front-surfaced mirror is placed $\frac{1}{2}$ in below lower end of tube at time of ignition

The operating procedure was as follows The tubes leading into the combustion vessel from the propane and air cylinders were filled with their respective gases Refer to Fig 1; stopcocks *a*, *b*, and *c* were opened, and stopcocks *d*, *e*, and *f* were closed The vacuum pump was started, and the lower end of the combustion tube was closed with a glass cover and a mercury seal After the system was evacuated, stopcock *a* was closed and the pump stopped (By observing the manometer, the system was checked for air leaks)